Preprint
UCRL-JC-147684

Density Distributions of Cyclotrimethylenetrinitramines (RDX)

D. M. Hoffman

This article was submitted to Joint Army Navy NASA Air Force 38th Combustions Subcommittee, 26th Airbreathing Propulsion Subcommittee, 20th Propulsion Systems Hazards Subcommittee, and 2nd Modeling and Simulation Subcommittee Joint Meeting, Destin, Florida, April 8-12, 2002

March 19, 2002

U.S. Department of Energy

Lawrence
Livermore
National
Laboratory

This work was performed under the auspices of the United States Department of Energy by the University of California, Lawrence Livermore National Laboratory under contract No. W-7405-Eng-48.

Density Distributions of Cyclotrimethylenetrinitramines (RDX)

D. Mark Hoffman
Energetic Materials Center
Lawrence Livermore Laboratory
Livermore, CA

Abstract

As part of the US Army Foreign Comparative Testing (FCT) program the density distributions of six samples of class 1 RDX were measured using the density gradient technique. This technique was used in an attempt to distinguish between RDX crystallized by a French manufacturer (designated insensitive or IRDX) from RDX manufactured at Holston Army Ammunition Plant (HAAP), the current source of RDX for Department of Defense (DoD). Two samples from different lots of French IRDX had an average density of 1.7958 ± 0.0008 g/cc. The theoretical density of a perfect RDX crystal is 1.806 g/cc. This yields 99.43% of the theoretical maximum density (TMD). For two HAAP RDX lots the average density was 1.786 ± 0.002 g/cc, only 98.89% TMD.

Several other techniques were used for preliminary characterization of one lot of French IRDX and two lot of HAAP RDX. Light scattering, SEM and polarized optical microscopy (POM) showed that SNPE and Holston RDX had the appropriate particle size distribution for Class 1 RDX. High performance liquid chromatography showed quantities of HMX in HAAP RDX. French IRDX also showed a 1.1°C higher melting point compared to HAAP RDX in the differential scanning calorimetry (DSC) consistent with no melting point depression due to the HMX contaminant.

A second part of the program involved characterization of Holston RDX recrystallized using the French process. After reprocessing the average density of the Holston RDX was increased to 1.7907 g/cc. Apparently HMX in RDX can act as a nucleating agent in the French RDX recrystallization process. The French IRDX contained no HMX, which is assumed to account for its higher density and narrower density distribution. Reprocessing of RDX from Holston improved the average density compared to the original Holston RDX, but the resulting HIRDX was not as dense as the original French IRDX. Recrystallized Holston IRDX crystals were much larger (3-500 μm or more) then either the original class 1 HAAP RDX or French IRDX.

Introduction

The Department of Defense (DoD) has a continuing interest in new and safer explosives for a wide variety of military applications. Recently SNPE, a French company, developed a proprietary method for making RDX with reduced shock sensitivity in cast cure formulations [1]. Dr. Pai Lu at the US Army's explosives research facility at Picatinney Arsenal headed up the effort to characterize this new IRDX under the FCT program. Some of the results from the IRDX FCT effort are given in references 2 - 10. Since shock initiation is believed to be associated with adiabatic heating of voids

in the explosive or density defects in the crystal [11, 12], density measurements of the explosive should at least correlate with and perhaps distinguish any RDX with improvement insensitivity to shock initiation from conventional RDX.

Two techniques are known to provide estimates of the density distribution of crystalline solids: (1) the density gradient method [13-16] and (2) the flotation method [17,18]. The density gradient technique was chosen because of its simplicity. The method requires two miscible fluids of higher and lower densities than the range of interest. Since the theoretical density of RDX is 1.806 g/cc [19], cesium chloride salt solutions with water were selected. Cesium chloride has a density of 3.988 g/cc and can be dissolved in water to a maximum solution density of 1.8689 g/cc so it was ideally suited for RDX density measurements. The salt is relatively inexpensive, can be recovered by evaporation and density values as a function of concentration are given in the CRC handbook [20].

Experimental

Initially the Army RDX samples were unavailable. Ken Hartman of Honeywell purchased an SNPE IRDX sample. H. Gokee of the Naval Surface Warfare Center kindly supplied a sample of this IRDX to us. This sample, designated C-416, was compared against two conventional samples of RDX. DSC, HPLC, light scattering particle size analysis, SEM, POM and the density gradient technique were used to characterize these three samples. When the three Army samples arrived, they were only evaluated by light scattering, density gradient and optical microscopy. Only class 1 RDX crystals were evaluated since fine particles are difficult to see and require long times to equilibrate in the density gradient column.

RDX samples. The six class 1 RDX samples evaluated in this work are listed in Table 1. Pai Lu supplied the Army samples (HRDX, SIRDX and HIRDX). One RDX sample was originally purchased from Holston (B-006) by LLNL and two were obtained from Indian Head (C-224 and C-416).

Table 1. SNPE and HDC RDX Class 1 crystal sample characteristics.

RDX ID	Lot #	Ave. Size (μm) (m)	T_m (°C)	Density (g/cc)	% TMD
B-006	HOL-21-44	200	204.6	1.783	98.73
C-224	IH 93095	150-175 (s)		1.770	98.01
C-416	S-	125 (s)	205.7	1.7966	99.48
H-RDX	HOL93K517-041	170 (m)		1.7887	99.04
H-IRDX	S800500	270 (m)		1.7807	99.15
S-IRDX	S085850	215 (m)		1.7951	99.40
H-RDX_2	HOL93K517-041	-	-	1.9848	98.83
H-IRDX_2	S800500	-	-	1.7923	99.24
S-IRDX_2	S085850	-	-	1.7957	99.43

s = SEM, m = laser light scattering; _2 after RDX ID indicates these experimental results are from Geo Centers by Karen Shaw.

Scanning Electron and Optical Microscopy. Scanning electron microscopy (SEM) was performed using a LEO 438 VP (variable pressure) SEM. The variable pressure SEM reduces surface charging of an organic sample by allowing a low-pressure atmosphere to pass over the sample [21]. This eliminated the need for a conductive surface coating. RDX crystals were sprinkled on an aluminum stud covered with carbon filled tape and examined without further preparation.

All polarized light microscopy was taken in transmission on a Leitz Aristophot microscope under crossed polars with a first order red plate. Optical micrographs were calibrated against photographs of a stage micrometer at the same magnification. RDX crystals were sprinkled on a microscope slide, coated with immersion oil and covered with a glass cover slip prior to observation.

Thermal analysis. A TA differential scanning calorimeter (DSC) model 2960 was used for the DSC scans. Scans were made at 10°C/ min. Sample size was approximately 0.5 mg.

Particle size distributions. A Malvern Microsizer Microplus small angle laser light scattering instrument was used for all particle size distribution measurements. The Malvern is designed to measure scattering intensity as a function of angle for suspensions of particles from 500 down to 0.05 μm using inverse Fourier optics. The main limitation of the instrument for class 1 RDX particle size distribution measurements was the 500-μm cutoff.

High Performance Liquid Chromatography (HPLC). The HMX content in RDX (B-006) and IRDX (C-416) was measured on 25 μl solutions in acetone. For each sample, two ~25 mg aliquots (weights recorded to 0.1 mg) were dissolved in 25 mL of acetone. Two aliquots of each solution were diluted 1:50 with a 50/50 mix of water/acetonitrile, and filtered. Each of the samples has an approximate concentration of 2 mg/L. Commercial standards (Aldrich) were used to prepare a series of standards (0.2, 0.5, 1.0, 2.0, 5.0, 10.0, 20.0 mg/L) in 50/50 water/acetonitrile. The samples and standards were sealed in auto sampler vials. No further processing of the samples or standards was performed.

A Hewlett Packard 1090 series II liquid chromatograph, controlled by HP Chemstation software, was used for this analysis. A 25 μL aliquot was injected onto an Agilent LiChrospher 100 RP-8 (5u, 4.0 x 100 mm) column (with a 4x4 mm RP-8 5μ precolumn) to perform reversed phase chromatography. A 10-minute isocratic run was performed with the following solvent mixture: 37% methanol, 63% water at 1.0 mL/min. HMX, and RDX were observed at 232 nm with a bandwidth of 4 nm, and reference at 520 nm. The retention times for HMX, and RDX were 1.9, and 3.2.

Density Gradient Method. A Techne model DC-2 density gradient column was used for all measurements. The column was immersed in a water bath with temperature controlled to 23 ± 0.05°C. The manufacture claims density can be estimated to 0.0001 g/cc with this equipment [15]. Filling device, platform, magnetic stirrer, two flasks and

connecting glassware are provided. A clearing device, consisting of a mesh basket that could be raised or lowered on a nylon thread by a motor, could not be used since the mesh in the basket was larger than the crystal size. Several attempts to modify this basket by reducing the mesh size were unsuccessful. Calibrated density floats for the range of interest, accurate to + 0.0002 /cc at 23°C, were used to calibrate the column. Figure 1 shows a schematic representation of the column and its various components. A column of varying density can be made by connecting two containers (4 and 5 in Fig. 1) in series to a large graduated cylinder (1) by a long smooth bore glass tube (6). The liquid is mixed in the second container and metered slowly into the column. Since the theoretical density for RDX is 1.806 g/cc, the liquid densities were approximately 1.75 and 1.81 g/cc. When the tube extends to the bottom of the graduated cylinder, the lower density fluid is added first and the higher density fluid is fed into the lower with continuous stirring. As new, higher density liquid flows into the column, the lower density liquid in the column is forced upward. When the column was full, the flow was stopped, the fill tube was carefully removed and calibrated glass density beads were added. The height of the center of each bead was measured to within 0.1 cm and a least squares calibration curve for the column was generated.

Several salts with high water solubility (listed in Table 2) were evaluated as possible density column solutions. Volume additivity was used to estimate the maximum density of the solution given in the table according to:

$$1/\rho = \omega_1/\rho_1 + \omega_2/\rho_2 \qquad (1)$$

where 1 and 2 represent solvent and salt, ρ is the density of the solution, solvent or salt and ω is the weight fraction of solvent or salt. As can be seen from the table, only CsCl and BaI_2 solutions have sufficiently high solubilities to allow solutions with higher density than RDX TMD to be prepared. Because of its cost and stability, CsCl was selected for all RDX measurements.

Table 2. Densities of various salt solutions

Material	Density	% in H_2O	Max soln den	Cost/kg
BaI_2	5.15	170	2.03	8K$
$BaBr_2$	4.781	104	1.67	$140
KI	3.13	127.5	1.616	$175
CsBr	4.44	124	1.750	1.2K$
CsCl	3.988	162.2	1.8689	$580

Estimates of CsCl density using volume additivity resulted in solution densities that were too high (see Figure 2). This makes reconstituting the solution after a set of density gradient measurements difficult. Fortunately, the CRC handbook [20] had data for CsCl density as a function of concentration in water at 20°C. When the data was fitted to a second order polynomial:

$$\rho = 1.1201\text{E-}2\omega^2 + 0.64335\omega + \rho_o \qquad (2)$$

where ρ_o = 0.99823 g/cc (water at 20°C) and ω is the weight fraction of CsCl, very accurate solution densities could be achieved and solutions could easily be reconstituted to a desired density once their density was known. Using distilled water allowed recovery of the CsCl.

The density gradient technique was a very convenient method for determination of density distributions for class 1 RDX crystals. About 0.01 g of crystals from a given lot of RDX are wetted with residual high-density fluid and added to the top of the column using an eyedropper. Crystals will generally fall through the density gradient liquid until their density matches the fluid density. This takes approximately 2 - 4 h for large (100 μm) crystals. The height of each individual crystal is read off the graduation marks on the column. Crystals of this size are relatively easy to see in the CsCl solution. Between 200 and 500 crystals were counted in each experiment over the height of the column. The height values are converted to density using the calibration beads and the density was summed from highest to lowest to generate a cumulative density distribution.

Results

I. Preliminary characterization:

Variable pressure SEMs of IRDX surfaces were only slightly smoother than conventional RDX surfaces from C-224 and B-006, see Figures 3-5. Neither of these RDX crystals had very good crystallographic faces. Since secondary electrons only penetrate 100 nm into the surface, internal defects cannot be observed using SEM. From the figures no large surface cracks were visible. If the crystals are transparent, polarized light microscopy (POM) is ideally suited for observing internal defects. Polarized light results are discussed with density gradient measurements.

As seen in Figure 6, HPLC measurements on conventional RDX (B-006) showed an HMX peak about 1.886 minutes into the run. IRDX (C-416) showed no HMX. It is well known that the Bachmann process, used to produce RDX in the US, yields small quantities of HMX [22]. The Woolwich process used in Europe to produce RDX yields almost no HMX, consistent with these HPLC results. It also appears that some HMX may act as a nucleating agent for RDX in the production of Class 1 RDX by HAAP. The concentration of HMX in B-006 RDX was 13.3 ± 0.4 weight percent.

When crystalline samples contain contaminants, a melting point depression proportional to the concentration of the contaminant is expected. In Figure 7 DSC measurements on C-416 IRDX and B006 RDX showed 1°C melting point depression in the RDX melting endotherm. Both imperfections and contaminants in crystals can have this effect. No effort was made to quantify the melting point depression. IRDX did indeed show a sharp melting endotherm characteristic of good crystals without contamination.

The average particle size of typical class 1 US RDX and French RDX as estimated from three runs on the Malvern Microsizer plus was 200 ± 7 μm (B-006) and 170 ± 13 mm (HRDX). The two samples of SNPE RDX gave similar average sizes (See Figure 8 for cumulative volume percents). However the reprocessed HIRDX was substantially larger, giving about 270 μm. It should be noted that the Malvern scattering apparatus used for these measurements has a 500 μm cutoff. This means that crystals larger than 0.5 mm are not counted by this technique. Missing the larger crystals would result in low estimates of the average particle size for the HIRDX samples. From our optical microscopy and measurements by others [2,3], crystals larger than 500 μm were observed only in HIRDX samples.

II. Density distributions in the 6 RDX samples.

Density gradient measurements showed IRDX (C-416) average density was 1.7966 g/cc (99.5% TMD). Figure 9 shows these results along with those for the other preliminary Holston RDX samples (B-006 and C-224). Similar samples were measured in a series of experiments at the French-German Research Institute of Saint-Louis (ISL) in France using the flotation density method [17]. The ISL data compared remarkably well with our density gradient technique for C-416 RDX as shown in the figure. For some reason, not explained in their paper, the ISL data was cut off at about 70% of the total distribution and was not measured above 1.8000 g/cc. Holston B-006 had an average density by the gradient method of 1.783 g/cc, 1.11% less than theoretical maximum. A third sample of Holston RDX (IH 93096L30GBP-133) obtained from the Naval Surface Warfare Center at Indian Head was even lower in average density (1.770 g/cc or almost 2% below TMD). The SNPE method produced crystals on average 0.6 to 1.5 % denser than production RDX crystals.

The second set of three class 1 RDX samples supplied by the US Army are shown in Figure 10. Again the ISL results are shown for comparison. The second SNPE RDX sample (SIRDX) gave an average density of 1.795 g/cc, very similar to the initial sample described in the preceding paragraph. However the density distribution of this sample was much sharper. This may be typical of lot-to-lot variation or reflect variability due to small sample size. The newer HAAP RDX sample gave 1.789-g/cc density, slightly higher than the older RDX sample (B-006). RDX can be made by continuous and batch processes which may account for this difference or it may also be lot-to-lot variation.

When the HRDX was reprocessed by SNPE to convert it to IRDX, the density distribution increased and the mean density increased to 1.791 g/cc (99.04 % TMD). Clearly, the French process for preparing IRDX was only partially successful in transforming the RDX from HAAP into IRDX of the same density as the original SNPE IRDX. Compositional analysis of the HIRDX [10] showed residual HMX in these samples. Granulation measurements [3] showed much larger class 1 HIRDX crystals compared to RDX and SIRDX. The breadth of the distribution was not as tight as the SNPE IRDX. The presence of HMX in the RDX is apparently responsible for the increase in granulation (crystal size) and the decrease in density observed when SNPE attempted to convert HRDX to IRDX using their proprietary process.

The density gradient methodology was transferred to Picatinny Arsenal and Karen Shaw of Geo-Centers made a second set of measurements on the three Class 1 HRDX, HIRDX, and SIRDX samples. The two sets of results are compared in Figure 11. In both sets of data the density varies such that $\rho(RDX) < \rho(HIRDX) < \rho(SIRDX)$. The average densities of the SNPE IRDX measurements were very similar (see Table 1). The HIRDX densities measured at Geo-Centers were slightly higher than those measured at LLNL. The conventional HRDX sample gave lower average density when measured at Geo-Centers. Since the sample sizes are only 10 mg, it is not surprising that such variations exist. Similar results are often observed in particle sized distribution measurements by light scattering. However the general results were consistent between both sets of measurements.

III. Polarized light microscopy

RDX, SIRDX and HIRDX polarized light micrographs are shown in Figures 12–14. An attempt was made to keep the magnification of each of the figures the same for ease of comparison. A first order red plate was used to facilitate observation of thin voids or inclusions that change the optical path length in of the transmitted light resulting in a color change. Since birefringent data on RDX is known [23], It should be possible to observe moderate size heterogeneous nuclei by changes in the optical properties.

As can be seen from Figure 12, there are several large inclusions or voids in HAAP RDX indicated by dark triangular or oval shaped spots inside the large RDX crystal. The crystal itself is about 375 x 270 μm and assuming the inclusions are not interconnected they vary in size from a few microns to almost 60 μm long by 15 wide. Thin elongated oval shaped sections were also observed as orange or blue structures due to addition or subtraction to the first order red plate (not shown in Figure 12) about the same dimensions as the dark inclusions described above. Finally a large number of quite small (1-2 μm) inclusions were found throughout these crystals.

Polarized light micrographs of the SNPE IRDX (SIRDX) showed substantially smaller thin voids or inclusions (some up to 20 μm long by 10 μm wide) in a crystal about 175 μm by 120 μm as shown in Figure 13. These thin voids or inclusions come in and out of focus as the optical microscope is adjusted to focus through the crystal, clearly indicating they are trapped beneath the crystal surface. In these preliminary observations there were no large dark central inclusions as seen in HRDX crystals such as the one in Figure 12. There were, however, numerous small (1-2 mm) dark inclusions similar to those found in the other RDX samples.

Some of the crystals of the Holston RDX that was recrystallized using the SNPE procedure (HIRDX) were more than 500 μm long, much larger then SIRDX! The large crystal in Figure 14 was 540 μm from end to end and 380 μm across. This crystal has smaller dark voids or inclusions near the center compared to HRDX in Figure 12. HIRDX also had the thin oval shaped colorful voids seen the SIRDX samples. There were also the numerous very small dark inclusions found in both other samples. Since

the large dark regions in or near the center of the HRDX and HIRDX samples were not seen in the SIRDX sample in these preliminary observations, they could contain HMX. This would explain the increase in size of the HRDX processed by SNPE. The effect of different solvents on RDX crystal morphology is just beginning to be understood [24,25]. Different processing techniques also have dramatic effects on explosive crystals, which are not completely understood [26]. If the original Holston RDX contains some HMX, because of its higher melting point, it would be expected to precipitate from solution first. If these small HMX crystals act as nucleating agents for the RDX, RDX crystallization would be heterogeneous, start more readily and tend to grow to larger sizes than SNPE RDX that contains no HMX. Assuming HMX acts as a nucleating agent, it should be incorporated near the center of the RDX crystal. Since the unit cells do not match, strains would occur as the RDX crystal grew, possibly leading to voids and cracks around the seed HMX crystal to accommodate the structural mismatch.

Discussion

From the microscopy and density measurements it is possible to estimate the number of voids required to produce the average density observed in the RDX samples if volume additivity and simple assumptions about the shape of the voids are made. Assuming the voids are all the same, the number of voids, n, is give by:

$$n = [1-(\rho/\rho_{tmd})](V_c/V_v) \qquad (3)$$

where ρ is the crystal average density measured by the density gradient, ρ_{tmd} is 1.806 g/cc, and V_c and V_v are the crystal and void volume, respectively. For the SIRDX crystal in Figure 13 assuming height equals width and a hexagonal shape yields a crystal volume of about 4 million cubic micrometers. If the voids in the SIRDX are approximated as cylinders with a length of about 1 μm, consistent with the focal length of an objective lens with a 0.18 numerical aperture [26] and a diameter of 15 μm, the void volume would be 700 μm^3 equation 1 yields about 33 voids per crystal of average density 1.7951 g/cc. When the edges of the crystal are allowed to make a 111 face (consistent with the orthorhombic unit cell [18]), the crystal volume goes down substantially (1.46 E6 μm^3) which reduces the number of voids in the crystal to about 12. In the crystal at the upper left of the figure, 15 or 16 of these voids can be counted.

In HIRDX these thin cylindrical voids were observed, but some larger or deeper voids can be seen in Figure 14. When these voids were assumed to be spherical (about 17.5 μm diameter) and the crystal hexagonal with width and height equal, the number of voids was 34 when the average density was 1.7908 g/cc. If the edges were allowed to slope, as above, the number of voids was reduced to 10. About 6-10 of these inclusions can be seen in the large HIRDX crystal in the figure.

Conventional HRDX, in Figure 12, showed larger dark voids than the HIRDX in Figure 14. When a void diameter of 36 μm was assumed, only 1 void of this size gave the observed average RDX density (1.7887 g/cc). However in the crystal at least 5 to 7

of these voids can be seen. Clearly these inclusions are not spherical and/or they contain entrapped material of some density other than zero. On closer examination of these voids, their tops and bottoms tend not to be in focus implying that they are more than 8 μm deep. They are not birefringent, nor do they yield addition or subtraction to the first order red plate when the crystal is rotated. These voids could contain HMX incorporated into the crystal. They could also be associated with multiple crystals growing together out of register. To determine the nature of these large deep inclusions, more work needs to be done. If HMX crystals were not incorporated in the RDX, they should be seen at the bottom of the density column since HMX TMD is 1.905 g/cc. This was not observed in either B-006 or HRDX samples.

Some work has been done with x-ray diffraction of good RDX crystals indicating central strain fields of a large growth defect [28]. Other workers have also recently reported a correlation between liquid pycnometry data and shock sensitivity [29]. An effort to model the effect of removing one or two RDX molecules from the lattice showed changes in the density of states of the crystal [30], but no estimate of void volume was given. It seems unlikely that such nanometer scale voids would be sufficiently large to form hot spots for initiation in the classical sense [11]. Our results have shown that in these RDX crystals there are voids or inclusions on a much larger scale that would be capable of forming classical hot spots. It appears that the French are well on the way to reducing the number and/or volume of voids in the large RDX class 1 crystals. It is surprising that the DoD has not emphasized recrystallization as a means of improving the defects in explosive crystals and thus their shock sensitivity.

Conclusions

In a preliminary evaluation of conventional RDX compared with new SNPE IRDX, moderate percentages of HMX were found in conventional RDX by HPLC. This impurity was responsible for a 1°C melting point depression of the RDX. Particle size distributions of both RDX and IRDX were similar and consistent with the DoD class 1 specification. SEM micrographs failed to show detailed internal structure. Density gradient techniques and optical microscopy were able to distinguish between RDX and IRDX.

The density gradient technique was able to distinguish conventional RDX from SNPE's insensitive RDX (SIRDX), and conventional RDX recrystallized with SNPE's method (HIRDX). The highest density RDX was made by SNPE at 1.7959 ± 0.0007 g/cc or 99.44% TMD. The distribution of SIRDX crystals measured using the density gradient method was remarkably similar to measurements made using the floatation method [17]. Recrystallized conventional RDX (1.7907 g/cc) was not as dense as SIRDX, but better than conventional RDX (1.770 - 1.7887 g/cc). The density of conventional RDX ranges from about 98% to 98.7% of its theoretical density.

Polarized light microscopy was a very useful tool for determining the nature and dimensions of the inclusions in the different RDX samples. SNPE IRDX contained mostly thin cylindrical voids about 10 to 20 μm in diameter by 1-2 μm deep. These data

and crystal dimensions were used to estimate the number of such voids in a crystal of average density at between 10 and 30. Actual count in one crystal was 12 inclusions of this type. Larger inclusions were found in RDX and the reprocessed HIRDX than the original SIRDX. This result is consistent with observed density differences. Larger volume inclusions in HIRDX resulted in a similar number of inclusions per crystal to those found in SIRDX. Very large voids in RDX were not spherical but probably concave and may have occurred along different crystal boundaries as two crystals grew together.

The variation in the density of conventional RDX and new SNPE IRDX is consistent with changes in shock sensitivity of cast cure explosives formulated from different samples. The void size is consistent with adiabatic compression of voids on the length scale of several microns. The density gradient method could be used as a quality control method to distinguish between the conventional and the insensitive RDX explosives.

Acknowledgements

Funding for these experiments provided by the US Army Foreign Comparative Testing Program under the direction of Dr. Pai Lu is gratefully acknowledged. Ing Chiu set up and ran the density gradient measurements and the HPLC measurement. Randy Weiss made the DSC measurements. Karen Shaw of Geo-Centers ran the second set of density gradient measurement on RDX, SIRDX and HIRDX when this test method was successfully transferred to the US Army at Picatinny Arsenal.

References:

1. A. Frenche, SNPE Memo to A. Melita Jan 3, 2000.
2. T. Dolch and B. Travers, "Safety Tests", FCT Program Team Meeting, May 1, 2001, Picatinny Arsenal.
3. G. Cheng, "Granulation", FCT Program Team Meeting, May 1, 2001, Picatinny Arsenal.
4. S. Moy and K. Klingaman, "IRDX for Gun Propellant" FCT Program Team Meeting, May 1, 2001, Picatinny Arsenal.
5. R. L. Stanley, "Evaluation of I-RDX as a Solid Rocket Propellant Ingredient", FCT Program Team Meeting, May 1, 2001, Picatinny Arsenal.
6. K.S. Burrows, "IRDX FCT – 155 mm IM PIP Program Support", FCT Program Team Meeting, May 1, 2001, Picatinny Arsenal.
7. S. Kerwien and D. Stec, III, "Microscopy of RDX: Holston, H-IRDX, S-IRDX", FCT Program Team Meeting, May 1, 2001, Picatinny Arsenal.
8. P. Baker, A Bines, W. Sunderland, R. Maulbetsch, and R. Cregar, "Electric Flyer Tests", FCT Program Team Meeting, May 1, 2001, Picatinny Arsenal.
9. D. A. Wiegand, "Search for Differences in the Surface Properties of RDX and IRDX by X-ray Photoelectron Spectroscopy (XPS)" FCT Program Team Meeting, May 1, 2001, Picatinny Arsenal.

10. E. Hochberg, "Chemical Analysis and Testing of RDX", FCT Program Team Meeting, May 1, 2001, Picatinny Arsenal.
11. C.M. Tarver, S.K. Chidester and A.L. Nichols, J. Phys. Chem., **100**, 5794 (1996).
12. R.W. Armstrong, H.L. Ammon, W.L. Elban, and D.H. Tsai, Thermochem. Acta, **384**, 303 (2002).
13. ASTM D 1505-85 "Standard Test Method for Density of Plastics by the Density-Gradient Technique"
14. Low, B.W. and Richards, F. M., "the Use of the Gradient tube for the Determination of Crystal Densities," J. Am. Chem. Soc., 74,, 1660 (1952).
15. Techne Operating Manual DC-1, DC-2, DC-3 and DC-4 (Feb. 1988).
16. L. H. Tung and W.C. Taylor, J. Polym Sci., XXI, 144 (1956).
17. L. Borne, J.-C. Patedoyl and C. Spycherelle, Propellants, Explosives, Pyrotechnics **24**, 255 (1999).
18. STANAG 4566 "Explosive Specification for ε-CL-20 (hexanitrohexaazaisowurtzitane) for Deliveries from one NATO Nation toAnother" Draft 8
19. C. S. Choi and E. Prince Acta Cryst., **B28** 2857 (1972).
20. CRC Handbook of Chemistry and Physics 67th ed. (R.C. Weast, ed.) CRC Press, Boca Ratan, FL (1987) pp. D-225-226.
21. J.I. Goldstein, D. E. Newbury, P. Echlin, D. C. Joy A. D. Romig, Jr., C. E. Lyman, C. Fiori, and E. Lifshin, "SEM and X-Ray Microanalysis", 2nd Ed. Plenum Press, New York, NY (1992).
22. Encyclopedia of Explosives **3**, (B.T. Fedoroff and O.E. Sheffield, eds). Picatinney Arsenal, Dover ,NJ, (1966) pp C 611-C 626.
23. W. C. McCrone, Anal. Chem., **22** 965 (1950).
24. J.H. terHorst, R.M. Gertman, and G.M. van Rosmalen, J. Crystal Growth, 230 277 (2001).
25. J.H. terHorst, R.M. Gertman, A.E. van der Heijden, and G.M. van Rosmalen, J. Crystal Growth 198/199 773 (1999).
26. U. Teipel, Propellants, Explosives, Pyrotechnics 24, 134 (1999).
27. E.M. Chamot and C. W. Mason, Handbook of Chemical Microscopy, John Wiley & Sons, Inc NY (1958) p. 14.
28. W.L. Elban, R.W. Armstrong, K.C. Yoo, R. G. Rosemeier, and R. Y. Yee, J. Mats. Sci., 24, 1273 (1989).
29. R.H.B. Bouma, A.C. Hordijk, A.C. vander Steen, T. Halvorsen and E. Skjold, "Influence of RDX crystal quality and size on the sensitivity of RDX based PBXs." Presented at 2001 IM & EM Tech. Symp. NDIA (November, 2001)
30. M. M. Kuklja and A. B. Kunz, J. Phys Chem of Solids, 85, 35, (1999).; J. Appl Phys, 85, 4428 (1999);

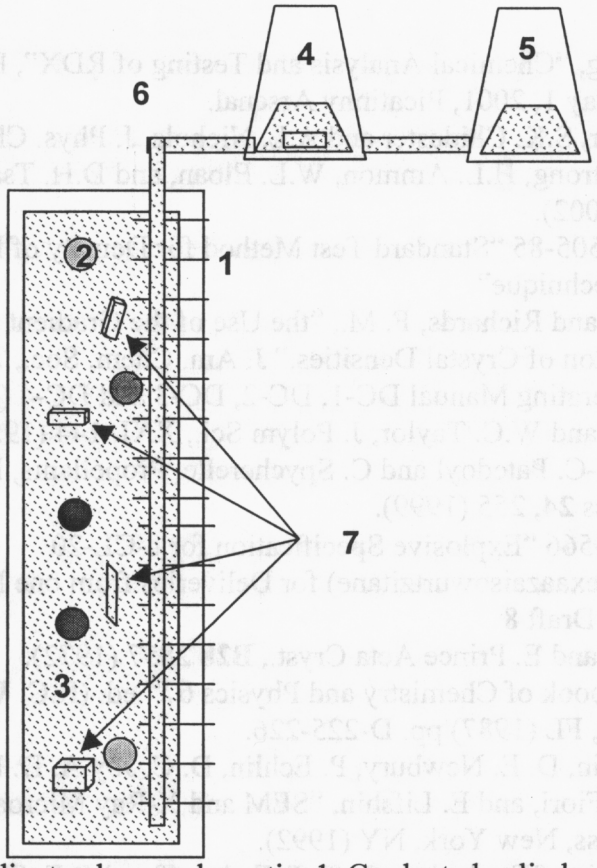

Figure 1. Density gradient column schematic: 1. Graduated cylinder, 2. Calibrated glass density bead, 3. Varying density fluid, 4. Low density fluid 5. High density fluid 6. Fill pipe (removed before measurements), 7. Crystals of different density.

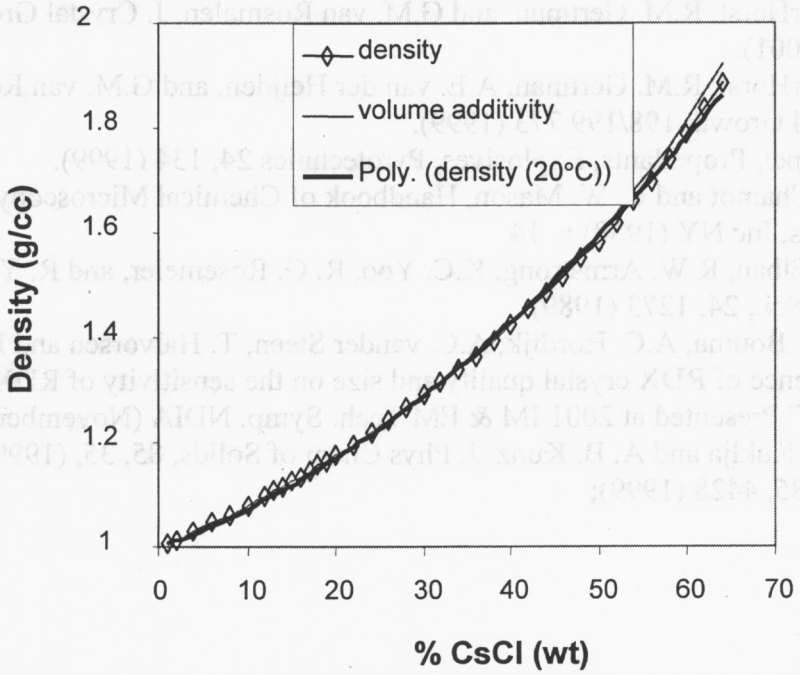

Figure 2. Solution density as a function of Cesium Chloride was fitted to a second order polynomial to aid in preparation of density gradient columns.

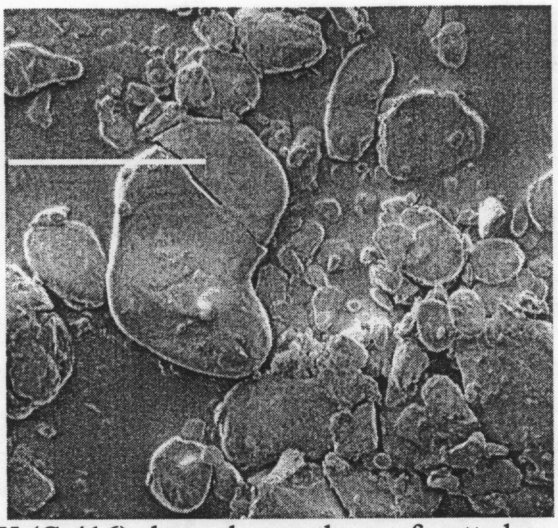

Figure 3. SEM of IRDX (C-416) showed smooth non-facetted surfaces without voids or cracks. (The crystal in the upper left was probably cracked during sample preparation.)

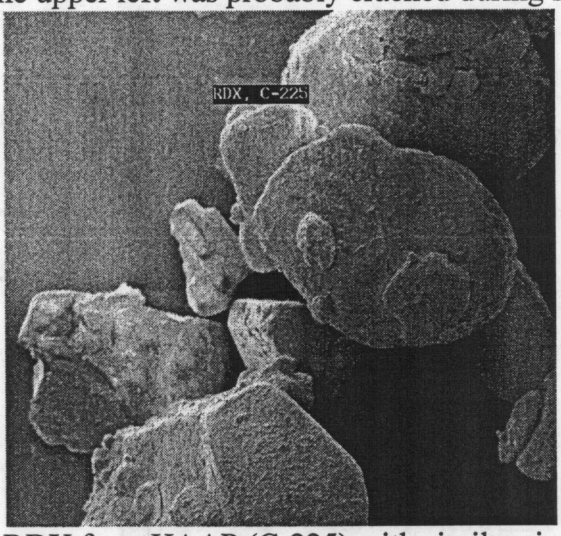

Figure 4 shows Class 1 RDX from HAAP (C-225) with similar size and surface characteristics to the IRDX in Figure 1.

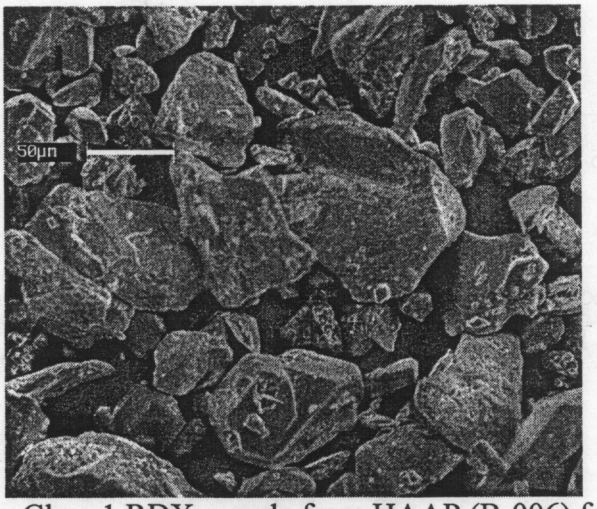

Figure 5 shows another Class 1 RDX sample from HAAP (B-006) for comparison.

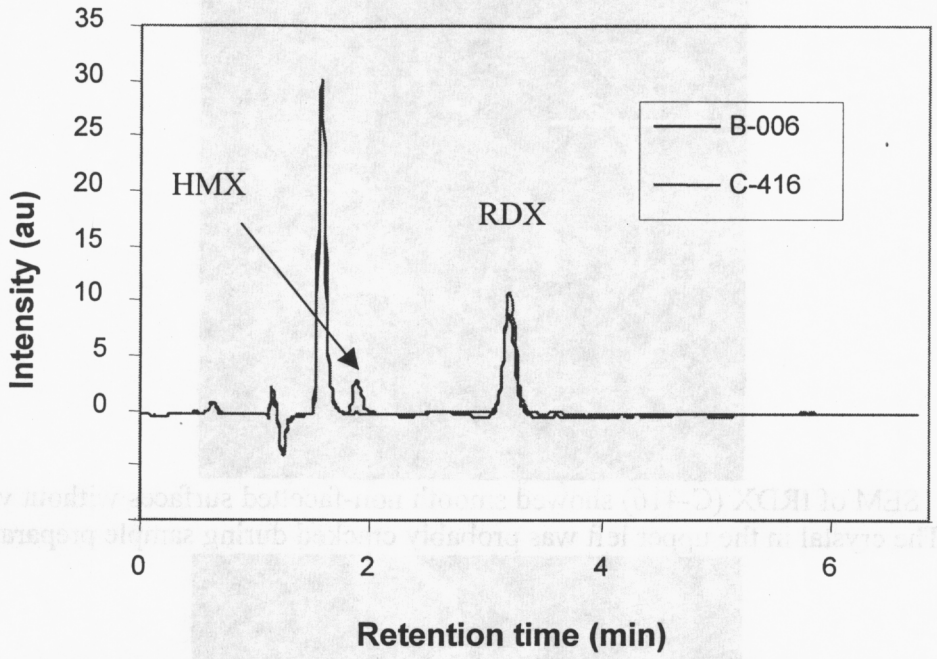

Figure 6 HPLC showed HMX contaminant in RDX but not IRDX (C-416).

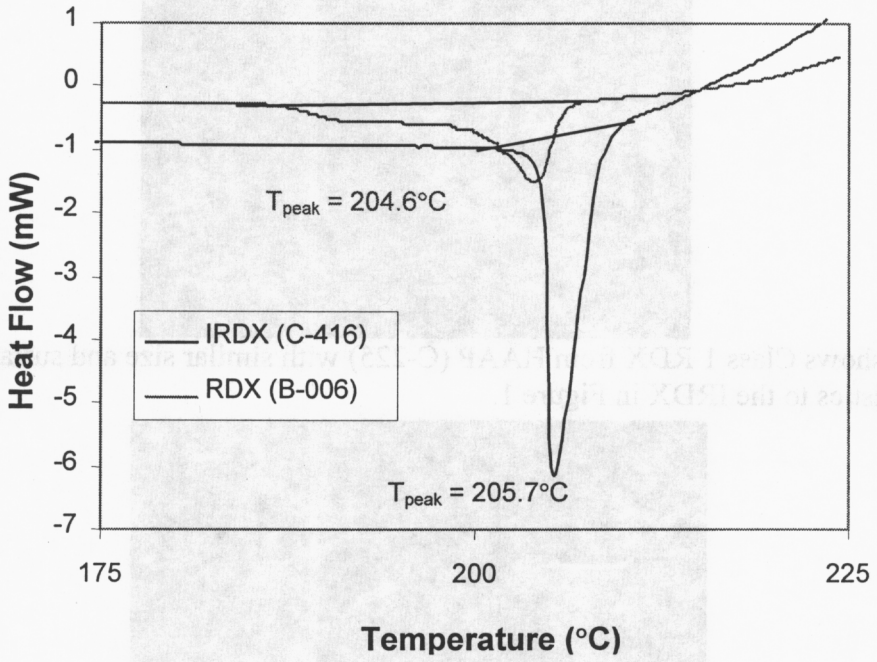

Figure 7. DSC traces of conventional RDX showed much broader endotherm and about 1°C lower melting peak temperature than IRDX.

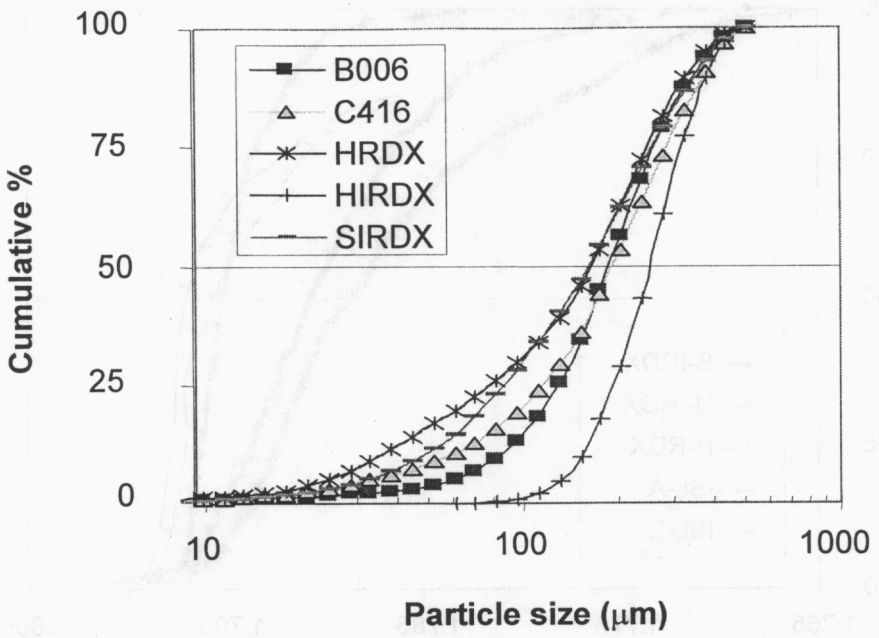

Figure 8. Cumulative particle size distributions for 5 "class 1" RDX's show substantial variation in average particle size. Results were between 170 and 270 μm. Note that the scattering apparatus cutoff was 500 μm

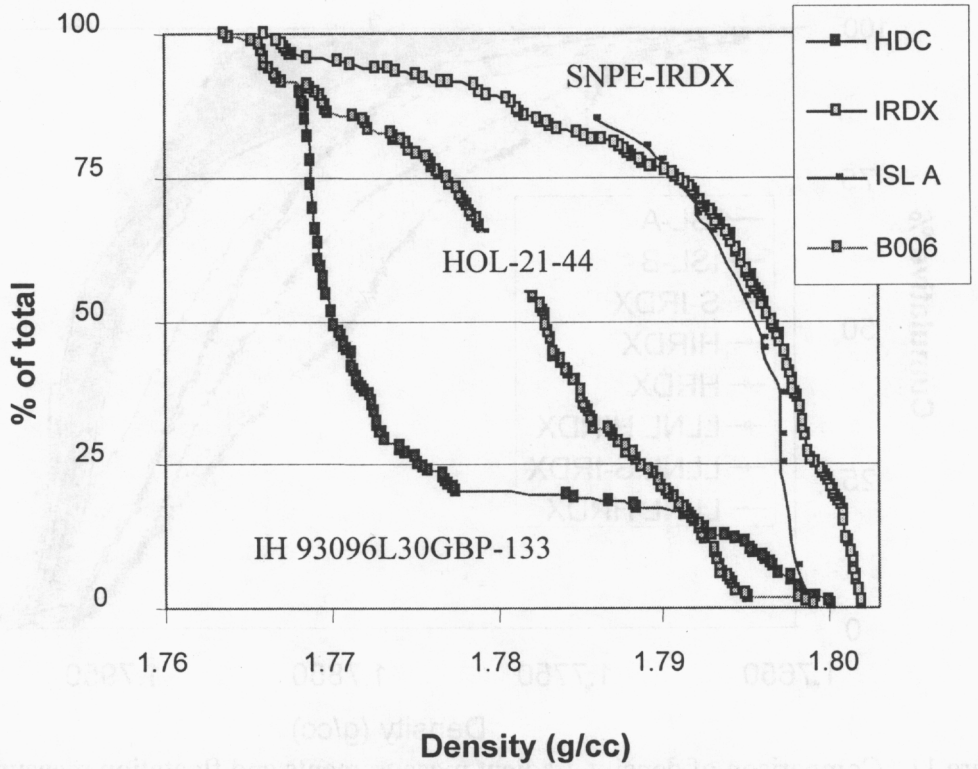

Figure 9. Preliminary density gradient measurements on three RDX samples showed substantial differences in density distribution.

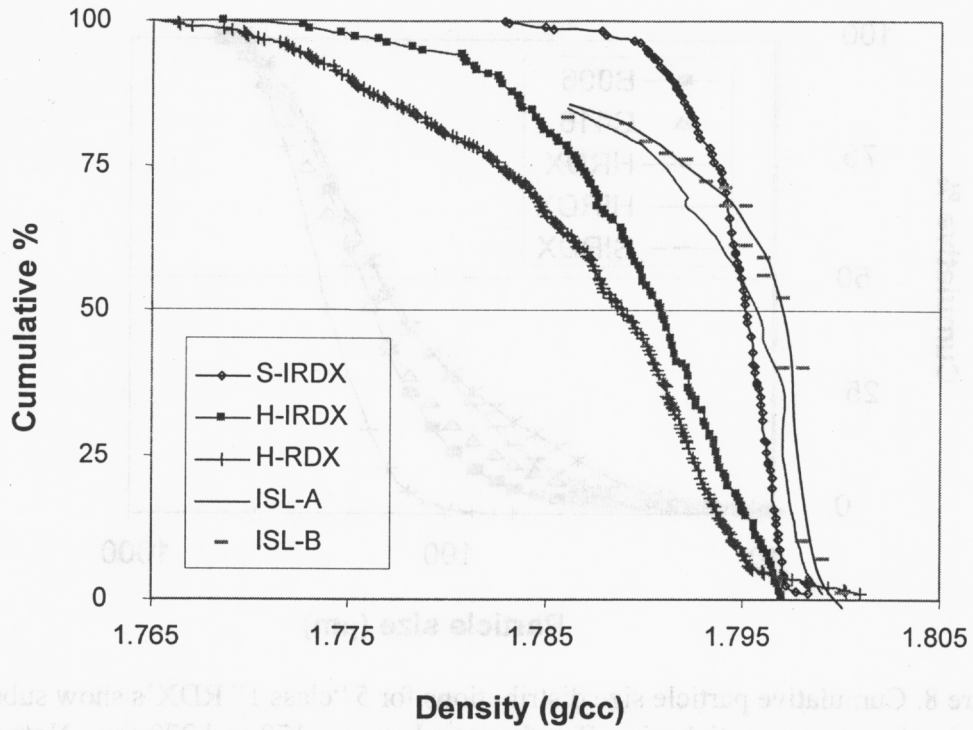

Figure 10. Density gradient measurements on various RDX samples compared to results from the literature based on the flotation method.

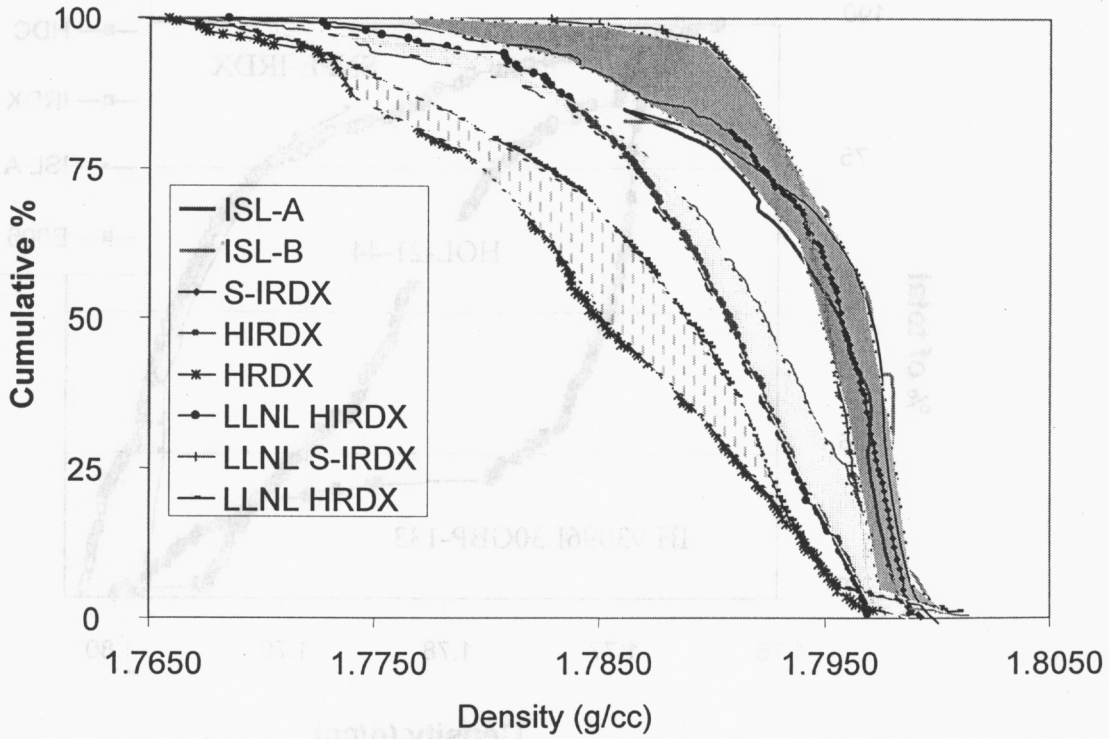

Figure 11. Comparison of density gradient measurements and floatation measurements on RDX, HIRDX and SIRDX show distinct ranges of density for each RDX type.

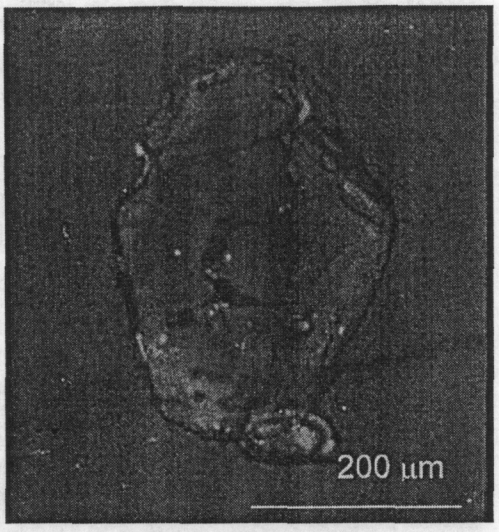

Figure 12. Polarized light micrograph of a large crystal of conventional RDX showed several large voids up to 125 μm long by 20 μm wide in a crystal about 325 μm by 250μm, somewhat larger than in the IRDX crystals.

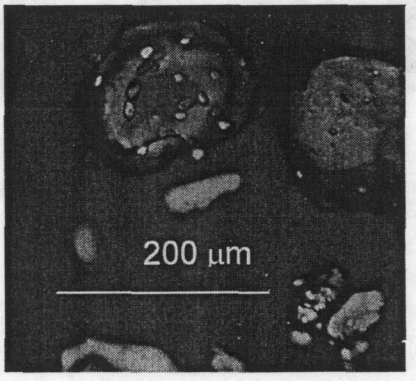

Figure 13. Polarized light micrograph of large crystals of SIRDX showed several thin, small voids up to 20 μm long by 10 μm wide in a crystal about 175 μm by 120μm, substantially smaller than those found in the conventional RDX crystals

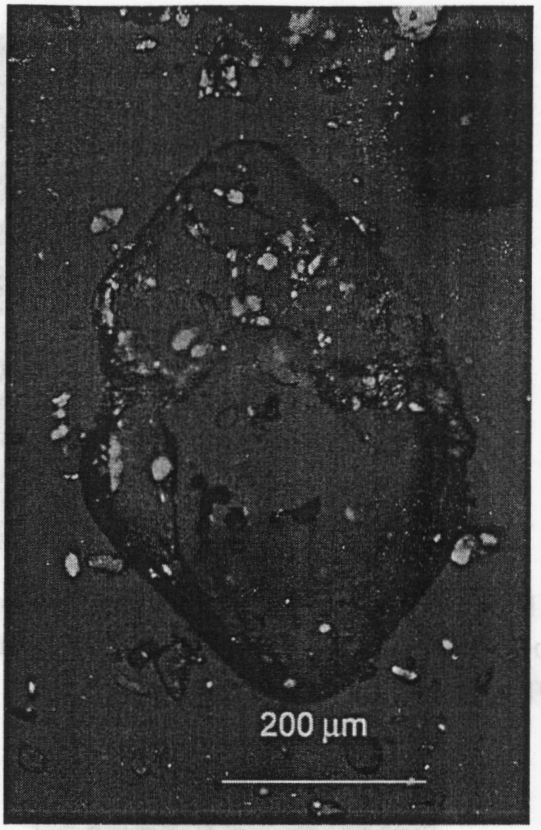

Figure 14. Polarized light micrograph of HIRDX showed several medium sized voids or possibly inclusions (10-25 µm across) inside a crystal about 400 µm by 600 µm in size.